Corticostriatal Contributions to Musical Expectancy Perception

Carol A. Seger, Brian J. Spiering*, Anastasia G. Sares
Sarah I. Quraini, Catherine Alpeter, James David,
and Michael H. Thaut

Abstract

■ This study investigates the functional neuroanatomy of harmonic music perception with fMRI. We presented short pieces of Western classical music to nonmusicians. The ending of each piece was systematically manipulated in the following four ways: Standard Cadence (expected resolution), Deceptive Cadence (moderate deviation from expectation), Modulated Cadence (strong deviation from expectation but remaining within the harmonic structure of Western tonal music), and Atonal Cadence (strongest deviation from expectation by leaving the harmonic structure of Western tonal music). Music compared with baseline broadly recruited regions of the bilateral superior temporal gyrus (STG) and the right inferior frontal gyrus (IFG). Parametric regressors scaled to the degree of de- viation from harmonic expectancy identified regions sensitive to expectancy violation. Areas within the BG were significantly modulated by expectancy violation, indicating a previously un- appreciated role in harmonic processing. Expectancy violation also recruited bilateral cortical regions in the IFG and anterior STG, previously associated with syntactic processing in other domains. The posterior STG was not significantly modulated by expectancy. Granger causality mapping found functional connectivity between IFG, anterior STG, posterior STG, and the BG during music perception. Our results imply the IFG, anterior STG, and the BG are recruited for higher-order har- monic processing, whereas the posterior STG is recruited for basic pitch and melodic processing. ■

INTRODUCTION

Music follows a complex syntactic structure. Multiple ele- ments (e.g., rhythm, melody, and harmony) are ordered by rules governing the sequential (horizontal) and simul- taneous (vertical) organization of sound patterns. These syntactic rules are implicitly acquired during develop- ment via environmental exposure (Pearce, Ruiz, Kapasi, Wiggins, & Bhattacharya, 2009) and differ between mu- sical systems; Western tonal music, one such musical sys- tem, underlies the forms of classical and popular music originating from Europe. We investigated harmonic pro- cessing by systematically manipulating musical pieces to follow or violate Western tonal conventions. These mu- sical pieces were presented to musically untrained young adults raised listening to Western tonal music. Our pri- mary goal was to examine BG involvement in processing harmonic expectancies. We predicted a role for the BG in harmonic processing based on functional neuroanatomy, computational considerations, and research in other cog- nitive domains demonstrating the BG's involvement in processing expectancies. Our second goal was to identify

cortical regions involved in harmonic processing, specifi- cally within the inferior frontal and superior temporal lobes. Our third goal was to examine how these cortical regions functionally interact with each other and with the BG during music perception using Granger causality mapping (GCM).

The role of the BG in harmonic processing has not been studied, although BG recruitment has been reported in some previous studies (e.g., Koelsch, Fritz, & Schlaug, 2008). Research focusing specifically on the BG and music has more commonly explored rhythm and tempo pro- cessing (Schwartze, Keller, Patel, & Kotz, 2011; Grahn & Rowe, 2009; Chen, Penhune, & Zatorre, 2008). However, there are a number of theoretical reasons to predict that the BG may play an important role in harmonic processing based on their functional neuroanatomy and findings from research in other cognitive domains. Neuroanatomically, the BG are a subcortical structure that interacts with cere- bral cortex via recurrent corticostriatal "loops." The BG modulate cortex activity via separate pathways (usually re- ferred to as direct, indirect, and hyperdirect) by affecting inhibition and excitation of cortical representations, thus allowing for selection or gating of specific representations, inhibition of alternative representations, and switching between representations (for more detailed reviews, see Braunlich & Seger, 2013; Seger, 2008). The BG are able

Colorado State University
*Present address: Department of Psychology, The University of Maryland.

to learn from experience which representations should be selected or inhibited via a dopaminergic feedback, a reward signal from the midbrain, that affects the degree to which corticostriatal synapses are strengthened (long-term potentiation) or weakened (long-term depression; Tritsch & Sabatini, 2012). The dopamine reward signal indicates unexpected reward or omission of expected reward (Bromberg-Martin, Matsumoto, & Hikosaka, 2010), which creates the potential conditions for learning. Reinforcement learning methods developed in the computer science field offer formal methods to characterize and quantify both measures of expectation (i.e., reward prediction) and violations of expectation (i.e., reward prediction error; Glimcher, 2011; Sutton & Barto, 1998). As a primary target of dopaminergic projections, the BG play an important role in coding these reward predictions and reward prediction errors. There are regional differences within the striatum. The dorsal striatum shows relatively greater activity for reward prediction, whereas the ventral striatum shows the strongest reward prediction error activity (Lee, Seo, & Jung, 2012; Seger, Peterson, Cincotta, Lopez-Paniagua, & Anderson, 2010).

We predicted the BG would be involved in harmonic processing, given the strong parallels between the BG's role in forming predictions and assessing prediction error and the similar functions inherent in musical harmony. One fundamental element of music is the manipulation of harmonic expectancy and violation of expectancy across sequences of musical events within a specific tonal system. Expectations are manipulated to create patterns of tension (when violated) and resolution (when the expected occurs). For example in the Western tonal system, moving away from a tonic chord develops tension but returning to the tonic creates release (Huron, 2006; Meyer, 1989). This idea led to the prediction that the BG would have a role in processing predictions and violation of predictions in music, similar to their role in other cognitive domains (Kranjec, Cardillo, Schmidt, Lehet, & Chatterjee, 2012; Zacks, Kurby, Eisenberg, & Haroutunian, 2011; Bahlmann, Schubotz, Mueller, Koester, & Friederici, 2009; Lohrenz, McCabe, Camerer, & Montague, 2007). Furthermore, theories of music learning argue tonal systems are primarily learned through experience (Krumhansl & Cuddy, 2010; Pearce et al., 2009; Tillman, 2008), which is consistent with the plasticity of the BG.

Much of the research establishing the role of the striatum in reward prediction and prediction error was performed using classical or instrumental conditioning tasks and their homologs (for review of these tasks, see Seger, 2009). These tasks typically use primary (e.g., food or water) or secondary (e.g., money or explicit verbal feedback) rewards. However, recent research has found that explicit external rewards are not necessary for prediction and prediction error processing: Similar activity occurs when expectations are formed and confirmed or violated even if the expected situation is not a primary or secondary reward. For example, in sequence processing, reward prediction error occurs when an unexpected item (e.g., a letter in an artificial grammar learning experiment) occurs (Bahlmann et al., 2009). This type of sequence processing is similar to harmonic processing in music; harmonic features are not primary or secondary rewards, yet they are subject to expectancy and violation of expectancy. Empirical studies have demonstrated that the BG are critical for developing expectations and responding to violations of those expectations across numerous additional domains, including social cognition (Schiffer & Schubotz, 2011), causal reasoning (Kranjec et al., 2012), counterfactual "might-have been" reasoning (Lohrenz et al., 2007), and event perception (Zacks et al., 2011).

The striatum is not a unitary structure: BG and cortex interact with each other within several dissociable corticostriatal "loops" (Haber, 2003; Alexander, DeLong, & Strick, 1986) that connect different regions of the cortex to different regions of the BG. We predict the BG will perform similar processes of prediction and prediction error processing within these loops, but the specific types of predictions will depend on the type of the representations within each respective cortical regions within a given loop. Although the corticostriatal system has no distinct borders separating loops, it is useful for heuristic purposes to conceptualize the system as containing at least four primary loops connecting striatum and cortex (Seger, 2008; Lawrence, Sahakian, & Robbins, 1998). The "motor loop" connects the putamen with motor and premotor regions of the frontal and parietal lobes. The "executive loop" connects the head of the caudate with lateral prefrontal and inferior parietal cortex. The "visual loop" connects posterior regions of the body and tail of the caudate with regions of extrastriate occipital and temporal lobes. The "motivational" loop connects the ventral striatum with OFC and other regions mediating reward and emotion. As described below, we predicted that harmonic expectancy might modulate activity in two important cortical regions: the inferior frontal gyrus (IFG) and superior temporal gyrus (STG). Specifically, we predicted the IFG and the head and body of the caudate would show similar harmonic expectancy recruitment and would functionally interact. This is based on the well-established anatomical connections between IFG and the anterior caudate (Haber, 2003; Alexander et al., 1986) and is consistent with Koelsch and colleagues' work (2008), which reported head of the caudate activity in a chord harmonic processing task that also activated the IFG. The connections between auditory regions of the superior temporal cortex and BG have been less well studied than other cortical regions. Yeterian and Pandya (1998) reported projections from the anterior STG to the dorsal anterior putamen and head of the caudate and projections from the posterior STG to the posterior putamen and body and tail of the caudate nucleus, and we therefore predicted that these corresponding regions would show similar recruitment by harmonic expectancy.

In conjunction with the BG, we were also interested in examining the role of the STG and IFG in harmonic processing.

The STG has been associated with processing sequences of tones and melodic structures (Klein & Zatorre, 2011; Lee, Janata, Frost, Hanke, & Granger, 2011; Rogalsky, Rong, Saberi, & Hickok, 2011). Musical processing in the IFG overlaps with regions involved in motor and linguistic sequencing (Levitin & Tirovolas, 2009; Janata & Grafton, 2003), and researchers have argued that this region contributes to syntactic and hierarchical processing in music (Patel, 2003). Previous research investigating musical harmonic expectancy has compared unexpected tonal chords (e.g., Neapolitan subdominants) to standard chords within a chord progression context. Neapolitan subdominants lead to an early right anterior negativity when studied using electroencephalography (Koelsch, Gunter, Wittfoth, & Sammler, 2005) and magnetoencephalography (Maess, Koelsch, Gunter, & Friederici, 2001) and activity in the right inferior frontal lobe when studied using fMRI (Koelsch, Fritz, Schulze, Alsop, & Schlaug, 2005; Koelsch et al., 2002). On the basis of this research, we predicted the IFG would be sensitive to musical expectancy. We did not make any predictions about the STG because previous research was unclear about its role in harmonic processing, with some researchers arguing that STG is limited to tonal processing, and others indicating a potential role of anterior STG regions in harmonic processing (see Koelsch, 2011, for a review).

To summarize, we examined, for the first time, the role of the BG in higher-order harmonic processing. We further investigated the role of the IFG and STG in harmony processing and examined interactions between these cortical regions using GCM. We predicted that the BG and IFG would be sensitive to harmonic expectancy violation, this sensitivity would be greatest in regions of the BG (i.e., head and body of the caudate) that interact with the IFG, and these regions would show functional connectivity during music perception. In addition, we predicted STG recruitment during music perception, along with regions of the BG (i.e., the putamen and posterior caudate) that interact with STG.

METHODS

Participants

Eleven participants (six men, five women) were recruited from the University of Colorado School of Medicine, Denver community. All participants met the criteria for MRI scanning (i.e., no metallic implants, no claustrophobia, and no known neurological injury or disease). All participants reported normal hearing and no history of neurological disorders or impairments that might affect musical processing. In addition, all participants reported no formal music theory training and no professional musical employment.

Stimuli

The stimuli were short, intact musical pieces. Choosing intact musical pieces improves ecological validity, in com-

parison with the isolated chords used in previous studies described above. Two authors with extensive professional musical training and composition experience (J.D. and M.T.) selected pieces and composed alternative endings that deviated to varying degrees from Western musical conventions. A total of 15 pieces written by European classical composers (e.g., J.S. Bach and Ludwig van Beethoven) were taken from keyboard instruction sourcebooks. Pieces varied in length from 10 to 24 sec when played. Popular pieces and excerpts from major compositions were avoided to minimize the chance of familiarity with the pieces among the participants.

Western music is based on tonality within key centers. The fundamental or starting pitch serves as the tonal center for a given key. Relationships in tonal space between keys can be determined by various systems of analysis (Krumhansl & Cuddy, 2010; Lerdahl & Jackendoff, 1996). We chose to use the circle of fifths, one of the most common systems, to characterize the degree of deviation in the stimuli. The circle of fifths is depicted in Figure 1. Janata et al. (2002) found different voxels within cortical regions were sensitive to different keys, indicating this tonal structure has some neural validity. Maps of tonal key space have been identified within the rostromedial pFC (Janata, 2009; Janata et al., 2002), the left IFG (Janata, 2009), and superior frontal gyrus (Alluri et al., 2012).

Cadences, a progression of notes that concludes a phrase, section, or piece of music, are one of the most central syntactic components in Western tonal music theory and composition; they enforce the sense of a central pitch or key center in a musical passage. One of the most common cadence configurations used to create a sense of closure to a passage, or a whole piece, is presenting the penultimate chord on the fifth scale degree (the dominant) above the fundamental pitch (the tonic) before proceeding to the tonic (e.g., G chord to C chord in the key of C). The
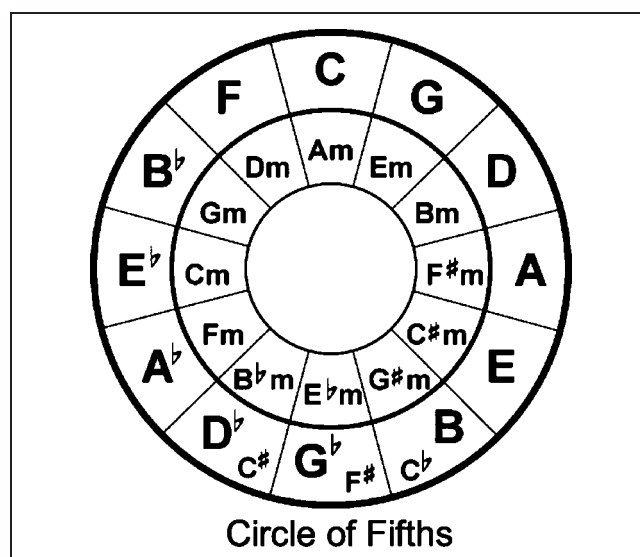

Figure 1. Circle of fifths.

penultimate chord creates a strong sense of expectation in Western music for the tonic to occur. Each stimulus piece's ending (the final cadence) closely followed standard tonal convention. In addition, each piece had a half cadence in the middle of the piece, followed by a repetition of the first half of the music that ended with a full cadence.

Three different types of musically realistic alternative cadences were written for each piece, each diverging to differing degrees from the cadence expectancies of Western tonal music. In addition to the Standard Cadence (i.e., original), we developed a Deceptive Cadence, a Modulated Cadence, and an Atonal Cadence. In the Standard Cadence, the ending cadence remained in the same key and resolved to the tonic chord; this is the most common resolution in Western tonal music and has a high degree of expectancy. In the Deceptive cadence, the piece modulated to a closely related key built on the submediant (the sixth scale degree from the tonic note); deceptive cadences are frequently used as a "surprise" device by replacing the expected final cadence, thus providing for the continuation of the piece. Deceptive cadences occur significantly less frequently than standard cadences and are not used to end a piece (Huron, 2006). In the Modulated Cadence, the piece modulated from the original key (e.g., C) to a new distant key via varying harmonic devices (i.e., a German sixth chord). These chords can be inserted within the middle of pieces to build additional compositional complexity but are never used as the ending cadence in Western tonal pieces. This cadence therefore has a lower expectancy than Deceptive Cadence. However, the piece remains within the harmonic space of Western tonal music. In the Atonal Cadence, the piece shifted into a series of chords that are not part of the "common practice" structure of Western tonal music; the final chord did not have a key center. All four versions of each piece were equated for number of notes and rhythmic properties. Thus to the greatest degree possible, only the harmonic structure of the piece was altered across cadences. An example piece with each of the four cadences is notated in Figure 2.

All 60 stimuli were validated by a separate group of 27 participants, who judged "How consistent is the ending?" on a scale from 1 (*very*) to 8 (*not very*). These participants were undergraduate students who participated in partial fulfillment of a research requirement for introductory psychology and were not selected on the basis of musical experience. Across all subjects and all pieces, the Standard, Deceptive, Modulated, and Atonal cadences received average ratings of 2.1, 4.4, 5.3, and 7.2 respectively, with 1 as the minimum and 8 as the maximum. A one-way within-subject ANOVA performed on the average ratings of each cadence for each participant indicated a significant effect of cadence, $F(3, 78) = 255, p < .0001$. Post hoc tests indicated that Standard received significantly lower ratings than Deceptive, $t(26) = 13.0, p < .0001$, Deceptive significantly lower than Modulated, $t(26) = 5.37$,

Figure 2. Top: A full piece with the Standard cadence (dashed box). Bottom: Deceptive, Modulated, and Atonal cadences for same piece.

$p < .0001$, and Modulated significantly lower than Atonal, $t(26) = 12.68, p < .0001$.

Procedure

Participants listened to a different musical piece on each of the 60 trials (i.e., each stimulus was presented only once). The order of the musical pieces was randomized with the restriction that same piece or cadence type would not be presented on two consecutive trials. Each piece was prerecorded and played on a digitally synthesized piano. When played, pieces ranged in duration from 10 to 24 sec. After the auditory presentation of each musical piece, the participants were visually probed with "Is the music pleasant? Yes or No." The probe question encouraged the participant to stay alert. Participants responded with their right index and middle fingers. A period of time was added after the probe question, during which no music or visual input was presented, to make the total duration of each trial 30 sec.

Auditory stimuli were presented to participants through a pair of magnet compatible headphones. Visual stimuli were presented to participants using a magnet-compatible projector that projects visual images onto a mirror attached to the radio-frequency (RF) head coil. Responses were

recorded via a magnet-compatible button box. A computer running E-Prime 2.0 experiment software (Psychology Software Tools, Inc., Pittsburgh, PA) was used to control stimulus presentation and interface with the magnet-compatible response boxes. Head movement was minimized using small foam pads placed on each side of the head inside the RF head coil.

fMRI Data Acquisition and Processing

Imaging was obtained with a whole-body 3.0-T MRI scanner (GE Healthcare, Milwaukee, WI) at the Brain Imaging Center at the University of Colorado Denver (Aurora, CO). The scanner was equipped with an eight-channel, high-resolution phased array head coil using GE's Array Spatial Sensitivity Encoding Technique (ASSET) software. Anatomical images were collected using a T1-weighted spoiled gradient recall sequence (minimal repetition time [TR], minimal echo time, inversion time = 450 msec, flip angle = 10°, field of view = 220 nm, 256 × 256 coronal matrix, 166 1.2-mm slices). The structural images were used to verify proper slice selection and to determine the sites of functional activation (i.e., voxels that were found to be significantly activated during the functional scan were overlaid on the high-resolution structural images). Functional images were reconstructed from 32 axial oblique slices obtained using a T2*-weighted EPI-gradient recalled echo sequence (TR = 2000 msec, echo time = 28 msec, flip angle = 70°, field of view = 220 nm, 64 × 64 matrix, 40-mm slices, no interslice gap) to measure BOLD signal change. In addition, the first three volumes, recorded before longitudinal magnetization reached a steady state, were discarded.

We chose to record BOLD signal continuously, and as a result, participants were exposed to scanner noise at the same time as the musical stimuli. However, we utilized high-quality magnet-compatible headphones, and all participants reported that they were able to hear the musical stimuli clearly above the scanner noise. We chose not to use a sparse sampling sequence, in which active scanning is limited to pauses between auditory stimuli, because it would have imposed constraints on our analysis. To model the BOLD signal both for the beginning of the piece (Music Baseline condition) and the endings (Standard, Deceptive, Modulated, and Atonal Cadence conditions), it was essential to record the BOLD signal during the entire stimulus presentation. A recent study comparing continuous scanning with sparse acquisition techniques during music perception reported comparable results for both methods in the regions of the brain we examined (Mueller et al., 2011).

Imaging preprocessing was performed using Brain Voyager QX 1.1 (Brain Innovation, Maastricht, the Netherlands). The functional data were first preprocessed (i.e., three-dimensional motion correction, slice time correction, temporal data smoothing with a high-pass filter, and linear trend removal). Each participant's high-resolution anatomical image was normalized to the Talairach and Tournoux (1998) brain template. The normalization process consisted of two steps: first, an initial rigid body translation into AC–PC plane and, second, an elastic deformation into the standard space performed on 12 individual subvolumes. The resulting set of transformations was applied to the participant's functional image volumes to form volume time course representations to be used in subsequent statistical analysis. Lastly, the volume time course representations were spatially smoothed with a Gaussian kernel FWHM of 6.0 mm.

Whole-brain Analyses

Brain Voyager QX 2.3 was used to analyze contrasts between conditions (Goebel, Esposito, & Formisano, 2006). First, a prototypical hemodynamic response function was convolved with the time course of the condition to create condition-specific models. Then, the condition-specific models were compared using the general linear model (GLM) with participants treated as random effects. We corrected for multiple comparisons using the cluster-size thresholding procedure developed by Forman et al. (1995), extended to 3-D maps, and implemented in the Brain Voyager Cluster Threshold plug-in (Goebel et al., 2006). An initial map was formed using an uncorrected voxelwise threshold of $p < .005$. Then, the minimum cluster size (on the basis of an alpha level of .05) was set by a 1000-iteration Monte Carlo simulation, simulating the stochastic process of image generation. Afterward, spatial correlations between neighboring voxels were calculated. Then, voxel intensity thresholds were calculated, and the corrected map was formed. The following six conditions were defined: Music Baseline, Silence Baseline, Standard Cadence, Deceptive Cadence, Modulated Cadence, and Atonal Cadence. The Music Baseline epochs began at the start of each musical piece and extended for a total of 3 TR (6 sec). The Silence Baseline epochs were defined as the last 2 TR (4 sec) of every trial. All cadence epochs (i.e., Standard, Deceptive, Modulated, and Atonal) were defined as the final 1–2 TR (2–4 sec) of music for each respective piece, depending on the specific length of the cadence within a given piece.

ROI Analysis

Our goal was an unbiased and conservative analysis to assess BG contributions to expectancy processing. To this end, we adopted a set of anatomically defined ROIs. These ROIs were previously defined for a different experiment (Peterson & Seger, in press), thus completely avoiding the possibility of biasing our anatomical ROI definitions by the functional analysis results. This ensured ROI definition independence and avoided issues of "double dipping," the statistically improper method of defining ROIs on the basis of a functional task and then further analyzing the

data within these ROIs (Kriegeskorte, Simmons, Bellgowan, & Baker, 2009; Poldrack & Mumford, 2009).

ROIs within the BG were defined a priori for the ventral striatum and three subregions of the dorsal striatum: the putamen, head of the caudate, and body of the caudate. These ROIs were hand drawn on an averaged image formed from the normalized high-resolution anatomical images from 10 participants. We manually verified the BG in this averaged anatomical image were comparable in size and shape to the averaged anatomical BG image from the participants in the present experiment. Care was taken to ensure only gray matter within each region was selected; any surrounding white matter or gray matter structures (e.g., thalamus) were excluded. The head of the caudate was defined as extending posteriorly through $y = 3$; the body of the caudate was defined as extending anteriorly through $y = 0$. A 2-voxel-wide gap was included between the ROIs to ensure independence. The ventral striatal ROI included the ventral caudate (nucleus accumbens) and ventral putamen, with the dividing line between the ventral and dorsal striatum extending along a diagonal from $z = 5$ in the most medial portions, down to $z = -4$ in the most lateral portions. All ROIs were then translated horizontally across the x axis to create complementary ROIs for the right hemisphere. These ROIs are illustrated in Figure 5. The ROI random effects GLM tool of BrainVoyager QX was used to analyze contrasts between conditions separately within each ROI.

Parametric Regressors

An a priori linear parametric regressor was defined to reflect the degree to which each cadence deviated from expected Western harmonic structure. We used the circle of fifths (see Figure 1) to determine the numerical distance between the original key and each modulated cadence. The distance was computed as the smallest number of steps between the roots of the original key and the final cadence within the tonal space of 12 major and 12 minor keys and then scaled to a range of 0.1 to 0.99, with the Standard cadence at .1 and the Atonal Cadence at .99. The Deceptive Cadence, modulating to a closely related key, resulted in a numerical value of 0.2. The Modulated Cadence, modulating out of original key via an augmented sixth chord, resulted in a value of 0.5. This parametric regressor was implemented in the same manner as the GLM used to perform the whole-brain analysis, described above.

We also formed a parametric regressor based on the average consistency ratings in the pilot testing of the pieces (described above), scaled to a 0 to .99 range. This resulted in weights of 0.16, 0.49, 0.62, and 0.89 for the Standard, Deceptive, Modulated, and Atonal cadences, respectively. Overall, these estimates are very close to those formed using the circle of fifths method. The largest discrepancy is for the Deceptive cadences, which were relatively close in tonal space (scaled value of 0.2)

yet received relatively high ratings for being inconsistent (scaled value of 0.49). Recent research in music is developing more sophisticated methods for calculating expectancy based on psychoacoustic methods, and future research may fruitfully incorporate these methods (Alluri et al., 2012; Janata, 2009).

GCM

GCM was used to explore effective connectivity between the striatum and other brain regions. The causality maps were created using Roebroeck, Formisano, and Goebel's (2005) procedure, as implemented within BrainVoyager QX 2.3. The first step in GCM is identifying reference regions, sometimes referred to as seed regions. Target regions were defined as any voxel not included in the reference region (y). Influence measures were then calculated from the reference to target region ($F_{X \to Y}$), target to reference region ($F_{Y \to X}$), and total linear dependence between the reference and target regions ($F_{X,Y}$) by repeatedly pairing the time course maps of each voxel in these regions. Time-course data were sampled from all trials. GCM analyses were performed on the preprocessed data, which included spatial smoothing. Directed influences to and from the reference region were calculated by subtracting the influence of the target to reference region from the influence from the reference to the target region ($F_{X \to Y} - F_{Y \to X}$) for every voxel to calculate a difference (dGCM). Thus, effective connectivity was described as dGCM = $F_{X \to Y} - F_{Y \to X}$ (see Roebroeck et al., 2005, for details). A positive difference value indicates $F_{X \to Y}$ (reference $\to$ volume) influence, whereas negative difference values depict $F_{Y \to X}$ (volume $\to$ reference) influence.

We focused on three cortical (IFG, anterior STG, and posterior STG) and two BG (caudate and putamen) seed regions. The cortical regions were functionally defined based on the All Cadences > Music Baseline contrast, shown in Table 2. We choose right hemisphere ROIs because they were more consistently active than the left hemisphere ROIs; however, exploratory analyses of left hemisphere ROIs found similar patterns. The right anterior putamen was functionally defined based on the All
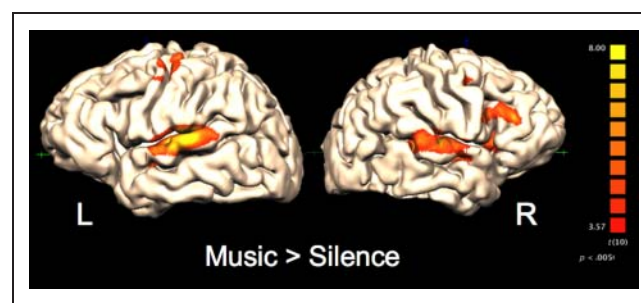

Figure 3. Regions with greater activity for Music Baseline than Silence Baseline. Positive *t* values are shown in orange–yellow scale. Corrected for multiple comparisons using the cluster level threshold method with a voxelwise threshold of $p < .005$ and cluster threshold of $p < .05$.

Table 1. Regions of Activity for Music

	x	y	z	Voxels
Music Baseline > Silence Baseline				
R STG	52	−20	5	16556
L STG	−53	−20	9	15444
R IFG	45	14	21	10231
Medial frontal/supplementary motor area	2	5	53	3411
R postcentral gyrus	49	−2	42	956
L postcentral gyrus	−48	−14	55	2332

x, y, z: Talairach coordinates of the central voxel within the activated cluster. Voxels: Size of cluster in voxels. R= right; L= left. Cluster size threshold minimum of 82 voxels based on corrected alpha $p < .05$, voxelwise alpha $p < .005$.

Cadences > Music Baseline contrast. The right caudate ROI was functionally defined based the results of the parametric regressor.

The right IFG ROI was centered at $x = 45, y = 23, z = −4$ and encompassed a total of 454 voxels. The right anterior STG ROI was centered at $x = 40, y = 17, z = −17$ and encompassed at total of 394 voxels. The right posterior STG ROI was centered at $x = 55, y = −20, z = 0$ and totaled 2502 voxels.[1] The putamen ROI was centered at $x = 17, y = 2, z = 6$ and encompassed a total of 314 voxels. The caudate ROI was centered at $x = 10, y = −1, z = 15$ and encompassed a total of 425 voxels. Individual effective connectivity maps were computed for

each ROI for each participant, then activation across maps were compared using a voxelwise t test examining whether activity was significantly different from zero, at a threshold of $p < .05$.

RESULTS

Overall Music Perception

As shown in Figure 3, extensive activations for music (Music Baseline > Silence Baseline) were found bilaterally in secondary auditory cortical regions extending along the STG. Music also recruited large regions of the

Figure 4. Top: Regions of activity for all Cadences compared with the Music Baseline (initial segments of musical pieces). Bottom: Regions of activity during cadence perception that were modulated by the parametric regressor scaled to cadence expectancy. Positive t values are coded by the red–yellow–orange color scale and indicate greater activity for Cadences than Musical Baseline (top) or activity that was positively predicted by the expectancy regressor (greater activity for greater violation of expectancy, bottom). Negative t values are coded in the blue–green–magenta color scale and indicate the opposite contrasts: greater activity for Musical Baseline than the Cadences (top) or activity negatively predicted by the expectancy regressor (less activity for a greater violation of expectancy, bottom). Multiple thresholds are indicated via different color scales. For positive t values, red indicates regions of activity meeting a voxelwise threshold of $p < .005$, corrected for multiple comparisons with the cluster level threshold method (cluster threshold $p < .05$); yellow indicates regions of activity meeting a voxelwise threshold of $p < .05$, uncorrected. For negative t values, these cluster thresholds are indicated by magenta and bright green, respectively. The transparent red–orange and blue–green color scales show unthresholded maps indicating t values that correspond to probability values ranging from $p = 0$ to $p < .05$. Ovals indicate corresponding regions recruited in the two analyses. Orange= anterior STG; magenta= posterior STG; cyan= inferior frontal/anterior insula; red= putamen; green= caudate.

Table 2. Regions of Activation for Cadences

|	x	y	z	Voxels
All Cadences > Music Baseline				
Cortical regions				
L superior frontal gyrus	−27	48	22	506
Medial frontal gyrus	2	38	34	1228
Medial frontal gyrus/supplementary motor area	−5	24	48	192
L anterior STG	−39	14	−18	307
R anterior STG	39	16	−18	219
L IFG/anterior insula	−44	14	−1	1057
R IFG	45	22	−3	217
L superior parietal lobe	−37	−58	59	1207
R inferior and superior parietal lobe	50	−40	44	6521
L inferior parietal lobule	−51	−41	37	222
Subcortical regions				
L cerebellum	−41	−32	−32	73
R anterior putamen	9	5	6	15
L putamen/insula	−32	−8	2	1220
Music Baseline > All Cadences				
R posterior STG	58	−27	8	595
R posterior STG	52	−15	2	625
L posterior STG	−53	−21	8	2384
R caudate (tail)	16	−42	22	497

x, y, z: Talairach coordinates of the central voxel within the activated cluster. Voxels: Size of cluster in voxels. R= right; L= left. Cluster size threshold minimum of 7 voxels based on corrected alpha *p* < .05, voxelwise alpha *p* < .005.

right IFG, including the right hemisphere homolog of Broca's area. In addition, music recruited neural regions associated with motor processing, including the bilateral sensorimotor cortex in the precentral and postcentral gyrus and SMA. The recruitment of both motor planning and execution regions is consistent with previous music and motor studies (Zatorre, Chen, & Penhune, 2007; Janata & Grafton, 2003). A complete list of active clusters can be found in Table 1. We also found regions of activity that were significantly more active during Silence Baseline than Music Baseline in medial regions of the frontal and parietal lobes (posterior cingulate/precuneus) and across higher-order visual cortical regions. The former regions are commonly active during relatively unstructured control conditions in neuroimaging studies and participate in a neural system often referred to as the "default network" (Andrews-Hanna, Reidler, Huang, & Buckner, 2010). Relative decreases in visual cortex activity are often reported when participants attend to an auditory task (Langner et al., 2012).

Cadence Processing

To identify neural regions associated with ending cadence-specific musical processing, we compared all cadence epochs (i.e., Standard Cadence, Deceptive Cadence, Modulated Cadence, and Atonal Cadence) with Music Baseline epochs (i.e., the first 6 sec of each piece). As shown in Figure 4 (top row) and Table 2, there was significant activation in several regions of the pFC, including the bilateral IFG. There was also activity in the bilateral anterior STG, a region that is known to have strong interconnections with the IFG and which is implicated in linguistic syntax processing (Friederici, 2009). There was also significant activity in parietal lobe regions and in the medial frontal gyrus. Subcortically, this contrast recruited regions of the cerebellum, the anterior putamen and head of the caudate (bilaterally), and the left posterior putamen and insula. The reverse contrast (Music Baseline > All Cadences) found increased posterior STG and tail of the caudate activity during the beginnings of the musical pieces in contrast with the

Figure 5. (Left) BG ROIs used in the parametric analysis. Yellow = putamen; blue = head of the caudate; purple = body of the caudate; red = ventral striatum. (Right) Beta weights within the BG ROIs for Standard Cadence, Deceptive Cadence, Modulated Cadence, and Atonal Cadence. *regions that were significantly modulated by the parametric regressor, $p < .05$; +regions with a trend toward modulation by the parametric regressor, $p < .1$. L = left; R = right; Put = putamen; Head = head of the caudate nucleus; Body = body of the caudate nucleus; VS = ventral striatum. See text for analysis details.
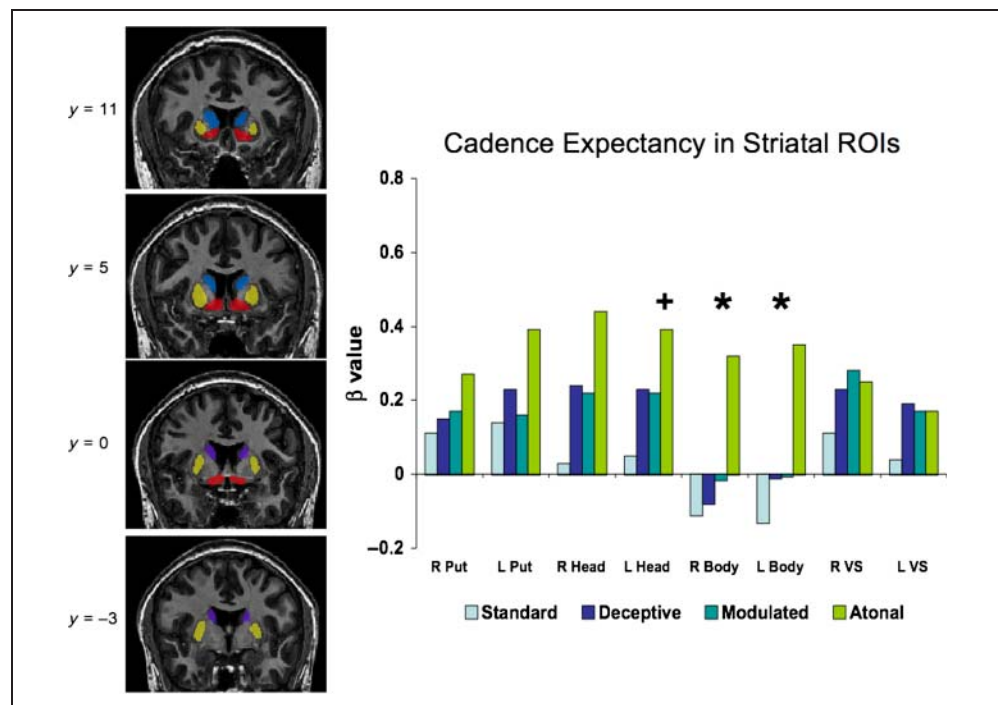
cadences. This unexpected pattern could reflect a variety of mechanisms, including increased analytical demands for processing tones at the beginning of a piece or habituation during extended musical processing.

Parametric Analysis of Cadence Expectancy

To identify neural regions sensitive to the degree of expectancy violation within the cadences, we utilized the parametric regressor based on the circle of fifths described above. Within the anatomically defined striatal ROIs, the regressor significantly predicted both right and left body of the caudate activity (right: $t(10) = 2.4, p = .03$; left: $t(10) = 2.1, p = .05$), with a trend toward predicting activity in the

right dorsal head of caudate ($t(10) = 2.0, p = .07$). This finding is illustrated in Figure 5.

We also incorporated the regressor in a whole-brain analysis to identify regions outside the BG significantly modulated by expectancy. This analysis indicated significant activity in the following cortical regions: the left anterior STG, the left IFG bordering on the anterior insula, and the supplementary motor region. This finding is illustrated in Figure 4 (bottom row), and significant clusters are listed in Table 3. Specific beta values within each of these three regions are shown in Figure 6. As shown in Figure 4, there was substantial activity in right hemisphere homologous regions at a lower statistical threshold. Overall, similar patterns of recruitment in bilateral IFG and

Table 3. Regions of Activity Predicted by Cadence Expectancy (Parametric Regressor)

	x	y	z	Voxels
Positive Relation to Parametric Regressor (Increased Activity with Increased Expectancy Violation)				
Bilateral thalamus/midbrain	0	−14	5	1211
Medial frontal gyrus/supplementary motor area	8	16	60	437
L IFG/anterior insula	−32	12	6	181
L anterior STG	−48	14	−12	488
Negative Relation to Parametric Regressor (Decreased Activity with Increased Expectancy Violation)				
Medial parietal/paracentral lobule	−3	−30	50	501
R inferior temporal gyrus	−53	−31	−22	723

x, y, z: Talairach coordinates of the central voxel within the activated cluster. Voxels: Size of cluster in voxels. R = right; L = left. Cluster size threshold minimum of 7 voxels, corrected alpha $p < .05$, voxelwise alpha $p < .005$.
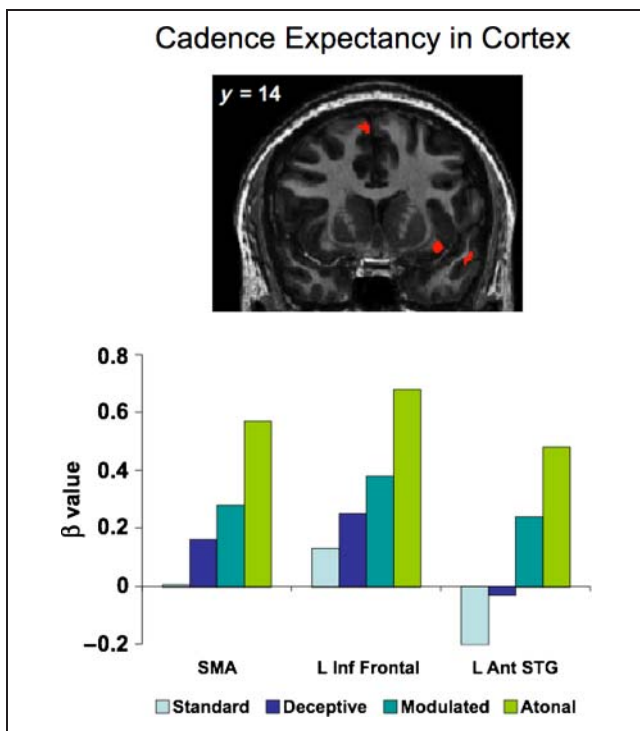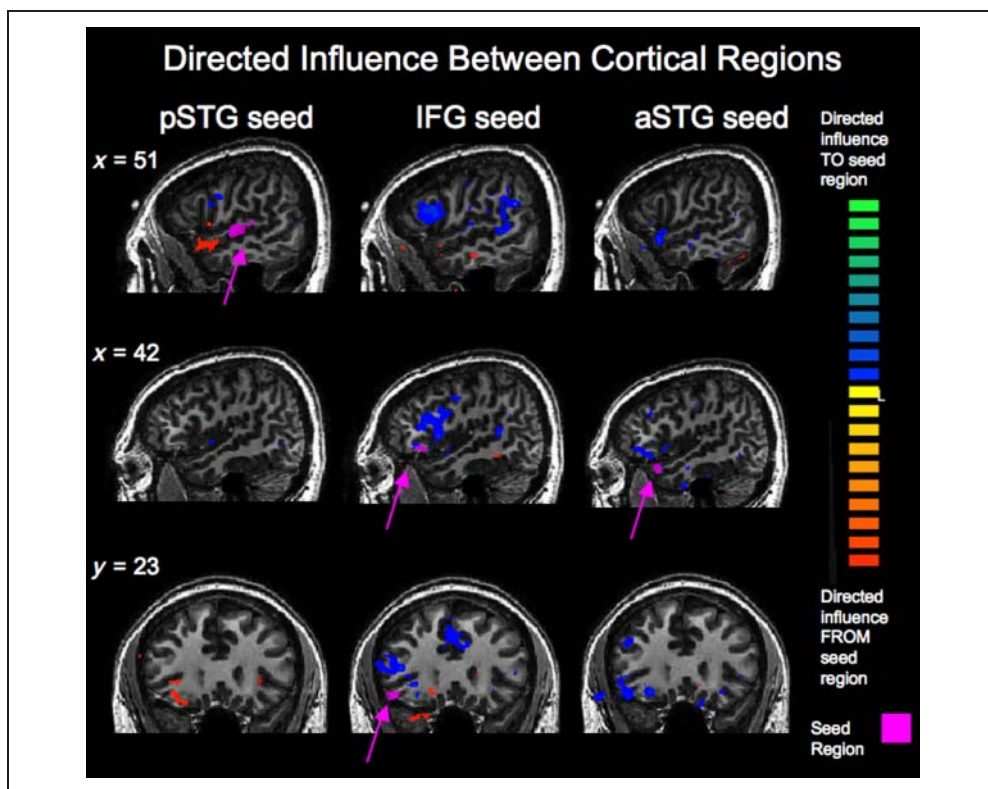
Figure 6. Activity within cortical regions identified in the whole-brain parametric analysis as significantly sensitive to cadence expectancy. Top: Regions overlaid on a coronal image at $y = 14$. Beta weights are plotted for the Standard Cadence, Deceptive Cadence, Modulated Cadence, and Atonal Cadence. SMA= supplementary motor area.

bilateral anterior STG, as well as in the putamen, can be seen by comparing the top (Cadences > Music Baseline contrast) rows to the bottom (the parametric regressor) rows of Figure 4. We found head and body of the caudate activity at the lenient threshold, consistent with the anatomical ROI analysis (see Figure 4, bottom row, slice at $z = 20$). There was a striking difference between the parietal and superior temporal lobes. The parietal cortex, bilaterally, was more active for cadences than early musical segments, yet there was little indication that it was modulated by expectancy. On the other hand, the posterior STG were more active for early music than for cadences and also showed little evidence of sensitivity to the expectancy violation regressor. Supplementary motor region recruitment for expectancy was not predicted, although a similar region was identified by Alluri et al. (2012) as negatively correlated with key clarity during music perception. It may reflect general processes of conflict detection and resolution within the medial frontal cortex (Nee, Kastner, & Brown, 2011).

In addition to the circle of fifths-derived regressor, we also implemented a parametric regressor based on the mean expectancy ratings made by a separate group of 27 participants (see above). Overall, the two sets of regressor weights were very similar: 0.1, 0.2, 0.5, and 0.99 for the circle of fifths weights, compared with 0.16, 0.48, 0.62, and 0.89 for the participant ratings weights. This regressor resulted in almost identical patterns of activity as found when using the circle of fifths derived regressor.

Figure 7. Directed influences to and from cortical seed regions in the right posterior STG (pSTG), right IFG, and right anterior STG (aSTG) as measured by GCM. Seed regions are shown magenta. Regions that the seed region exerted directed influence on are shown in warm colors, and regions exerting directed influence on the seed region are shown in cool colors. Overall, the pSTG exerted directed influence onto the IFG and aSTG (left column). The IFG (middle column) received directed influence from the pSTG and nearby regions of the frontal cortex. The aSTG (right column) also received directed influence from nearby regions of the frontal cortex.

Figure 8. (Top) Directed influences to and from the anatomically defined R body of the caudate seed region (see top left slice for seed region location). The body of the caudate interacted with other regions of the striatum in that it received influence from the putamen and exerted influence on other parts of the caudate nucleus (best illustrated in the top left image; the top right and bottom left also show the directed influence on the head and tail of the caudate, respectively). The body of the caudate also received directed influence from the posterior STG and IFG. (Bottom) Directed influences to and from the cortical seed regions shown in Figure 7 within the caudate and putamen. The putamen exerted directed influence on all three seed regions, whereas the caudate received directed influence from the IFG and anterior STG.

GCM

We examined patterns of directed influence from the following five seed regions in the right hemisphere: the posterior STG, the IFG, the anterior STG, the anterior putamen, and the caudate. The defining procedures for these seed regions were discussed above. Although we focused on the right hemisphere seed regions, similar directed influence patterns were found for left hemisphere seed regions. We found directed influence from the right posterior STG onto the IFG and adjacent regions of the STG, including the anterior STG (Figure 7, left column). There was also directed influence from small regions of bilateral primary motor cortex and to the left anterior STG and cerebellum. We found interaction

between right posterior STG and the BG. Specifically, there was directed influence from the putamen (Figure 8, bottom left) and directed influence to the ventral striatum (not illustrated).

There was directed influence onto the right IFG region from adjacent regions of the IFG and middle frontal gyrus in the right hemisphere as well as homologous regions in the left hemisphere. The right IFG showed directed influence both from and onto small regions of the anterior STG in both hemispheres. There was directed influence from the posterior STG bilaterally, consistent with posterior STG seed results. There was also directed influence from the bilateral inferior parietal regions around the angular gyrus, which is consistent with the known interactions between inferior parietal and IFG during verbal and auditory working memory (Burzynska et al., 2011). Finally, there were directed influences from the putamen and onto the caudate (Figure 8, bottom center).

The right anterior STG seed region exerted directed influence onto adjacent regions of the anterior STG and inferior and middle frontal regions in both hemispheres (Figure 7, right column). Interactions between right anterior STG and the BG were similar to those for the IFG seed: The anterior STG received directed influence from the putamen and exerted directed influence on the caudate (Figure 8, bottom right).

The patterns of directed influences between cortex and each of the two BG seed regions differed substantially, as shown in the top two rows of Figure 8. The putamen seed region exerted directed influence on the posterior and anterior regions of the superior temporal lobe, the TPJ, and the caudate nucleus. The caudate seed region, which was at the junction of the head and the body of the caudate, showed directed influence from several frontal cortex regions, including the bilateral IFG, bilateral dorsolateral pFC, and bilateral medial pFC. Within the striatum, the putamen seed exerted directed influence on the caudate nucleus, and the caudate seed received directed influence from the putamen and exerted directed influence on other regions of the caudate. The directed influence from putamen onto the caudate has been found previously in our lab in category learning tasks (Lopez-Paniagua & Seger, 2011; Seger, Dennison, Lopez-Paniagua, Peterson, & Roark, 2011; Seger et al., 2010), but this is the first time this putamen–caudate interaction has been reported in another cognitive domain.

Both the putamen and caudate seed regions received directed influence from large regions of the cerebellum; it is unclear what functional role these interactions may have in music perception. There is a growing literature concerning the roles of the cerebellum in music perception, with many studies indicating a role in temporal properties of music (Lebrun-Guillaud, Tillmann, & Justus, 2008), including rhythm processing (Chen et al., 2008) and auditory–motor synchronization (Thaut et al., 2009). It is less clear

whether the cerebellum plays a role in tonal properties of music, though studies have found a potential role in pitch perception (Parsons, Petacchi, Schmahmann, & Bower, 2009).

DISCUSSION

We found regions of the BG, in particular the anterior caudate nucleus, and cortex, in particular the IFG and anterior STG, were modulated by expectancy violation during music perception. The bilateral posterior STG were active for music but were not sensitive to expectation violation. Our results are consistent with music theories that argue music requires processes of structural development in which expectancy increases and resolution in which the expectancies are confirmed (Huron, 2006; Meyer, 1989).

The BG in Harmonic Expectancy Processing

BG's sensitivity to musical expectancy violation was predicted by reinforcement learning theories that propose BG networks represent both reward prediction and prediction error (Glimcher, 2011). This is consistent with previous findings of BG recruitment for prediction and prediction error in other cognitive domains, including reasoning (Kranjec et al., 2012; Lohrenz et al., 2007), sequence processing (Bahlmann et al., 2009), and event perception (Zacks et al., 2011). Our results provide convergent evidence from music for the general role of the BG in both reward prediction and reward prediction error.

Within the BG, both the anatomical ROI analysis and whole-brain analysis indicated significant recruitment during expectancy violation was localized to the body and head of the caudate. Our ROI analysis further showed a common, but nonsignificant, general pattern of expectancy sensitivity across all regions of the striatum (see Figure 5). The parallel pattern of activation of head and body region of the caudate along with the IFG is consistent with the known interaction pattern within the "executive" corticostriatal loop. In addition, GCM showed directed influence from frontal cortical regions to the right caudate seed region. The putamen showed a similar pattern of activity: activation in the All Cadences > Music Baseline contrast and modulated by the parametric regressor at a lenient threshold. However, GCM found a very different pattern of functional connectivity for the putamen than the caudate. The putamen interacted with the anterior and posterior superior temporal regions, consistent with anatomical connections between these regions (Yeterian & Pandya, 1998). Finally, the All Cadences > Music Baseline contrast revealed regions of the tail of the caudate that were more active for the beginnings of the pieces of music than the ending cadences but was not notably affected by the expectancy regressor; this same pattern of activity was found in the

posterior STG, known to project to the tail of the caudate (Yeterian & Pandya, 1998).

We did not find significant modulation of the ventral striatum by expectancy (although Figure 5 does show a small trend toward less activity for the Standard cadences compared with the other cadences). This result is in contrast to studies that have found ventral striatal activity associated with the rewarding and pleasurable aspects of music (Montag, Reuter, & Axmacher, 2011; Vuust & Kringelbach, 2010) and that found dopamine release in the ventral striatum associated with listening to musical segments selected by subjects individually as being intensely rewarding and emotional (Salimpoor, Benovoy, Larcher, Dagher, & Zatorre, 2011).

Our findings of BG recruitment during harmonic processing have implications for both the fields of BG research and musical neuroscience. BG research would benefit from the continued exploration of music as a specific instantiation of the more general prediction functions of the BG. Examination of expectancies across musical domains (e.g., rhythm, melody, and harmony) may provide insights into the roles of different corticostriatal loops. Given the BG's highly plastic nature, they play an important role beyond representing expectations within the current environment to learning what to expect in the future (Frank, 2011; Ashby, Turner, & Horvitz, 2010; Seger, 2009), which may have implications for theories of music acquisition.

The Inferior Frontal Lobe and Anterior STG in Harmonic Processing

The IFG has three main subregions: the frontal operculum bordering on the anterior insula (classic Broca's area, often identified as BA 44), an immediately anterior region (often identified as BA 45), and an immediately inferior region (often identified as BA 47). All three of these areas, in the right hemisphere, were active when comparing music to silence, but their activity was limited to the inferior region in our analyses of cadences and cadence expectancy. Our results are dissimilar from previous studies, comparing standard chord progressions with unexpected Neapolitan subdominant chord progressions, which found broad inferior frontal lobe recruitment for unexpected chord progressions (Koelsch, Fritz, et al., 2005). This inferior frontal lobe recruitment was associated with ERAN (Early Right Anterior Negativity) modulation, an ERP shown to originate in right frontal cortex (Garza Villarreal, Brattico, Leino, Ostergaard, & Vuust, 2011; Maidhof & Koelsch, 2011; Koelsch, Gunter, et al., 2005; Maess et al., 2001). Neapolitan subdominants rarely appear in Western tonal music, and although they are consistent with its tonal structure, they require a specific harmonic context to make syntactic sense.

It is still unclear how inferior frontal regions differ in their contributions to music processing. Both natural language and artificial grammar studies found evidence for a posterior (less complex hierarchy) to anterior (more

complex hierarchy) processing gradient within the inferior frontal region (Perani et al., 2011; Santi & Grodzinsky, 2010). In addition, more anterior regions are recruited to process syntactic dependencies across longer lags (Bahlmann et al., 2009; Bahlmann, Schubotz, & Friederici, 2008; Opitz & Friederici, 2007). BA 47 was recruited during polyrhythm hierarchical processing (Vuust, Wallentin, Mouridsen, Ostergaard, & Roepstorff, 2011). The inferior frontal region is important for verbal working memory and the articulatory loop (Groussard et al., 2010), and it is possible that cadences with higher degree of expectation violation have increased working memory demands. The IFG is active during melodic working memory tasks (Jerde, Childs, Handy, Nagode, & Pardo, 2011; Schulze, Zysset, Mueller, Friederici, & Koelsch, 2010). However, language studies found this region makes contributions to syntax that extend beyond working memory (Makuuchi, Bahlmann, Anwander, & Friederici, 2009).

A similar sensitivity to cadence expectancy was found in both anterior STG and IFG. Previous music studies have not distinguished between the contributions from these two regions. In the domain of language, the anterior STG has been associated with syntactic processing (Brennan et al., 2012). Anatomically, the anterior STG region is highly interconnected with the IFG (Friederici, 2009). Some studies (Friederici, 2009), but not all (Wilson et al., 2011), have related individual differences in syntactic processing ability to differences in white matter connectivity within this pathway. Our results imply that the anterior STG may play a role in processing musical as well as linguistic syntax and the musical processing functions of the anterior STG differ from those of the posterior STG, which was not sensitive to harmonic expectancy in the current study.

Functional Connectivity across Frontal, Temporal, and Striatal Regions

We found that both anterior STG and IFG were sensitive to expectancy. GCM provided convergent evidence for the presence of this functional interaction: Seed regions in both anterior STG and IFG indicated functional connectivity between these two regions. GCM also indicated functional connectivity between the posterior STG and IFG and anterior STG. Interactions between IFG and the STG are consistent with studies of congenital amusia that find decreased gray matter in both regions along with decreased white matter in the tracts connecting the two regions (Hyde, Zatorre, & Peretz, 2011; Peretz, Brattico, Järvenpää, & Tervaniemi, 2009). In addition, white matter connectivity in this pathway is associated with the ability to learn new syntactic structures in the auditory domain (Lopez-Barroso et al., 2011; Loui, Li, & Schlaug, 2011) and increased white matter connectivity is found in these tracts after intensive melodic intonation therapy for nonfluent aphasia (Schlaug, Marchina, & Norton, 2009).

GCM also supports the presence of functional interaction between anterior STG, posterior STG, IFG, and

BG during music perception. Overall, these interactions were consistent with the known anatomical connections between cortex and BG within corticostriatal loops. The putamen interacted with the STG, whereas the caudate interacted with the IFG.

GCM results should be considered within the methodology's limitations. First, GCM influence measures do not necessarily reflect a direct anatomic connection between regions; GCM does not discriminate between direct connections and indirect influences through a third region. Second, recent fMRI simulations have indicated that all functional connectivity techniques, including GCM, have limited ability to accurately determine the direction of influences (e.g., whether region A is causing activity in region B or vice versa; Smith et al., 2011).

Characterizing the Roles of Frontal and Temporal Regions

The current study contributes to the emerging view that early music perception recruits the posterior STG and later perception recruits anterior regions of the anterior STG and IFG. In addition to the GCM results, this view is supported by ERP studies finding an early MMN in temporal sites and a later ERAN in frontal sites (Garza Villarreal et al., 2011; Doeller et al., 2003). The posterior STG appears to be recruited for individual pitch processing and chord processing (Fujisawa & Cook, 2011; Klein & Zatorre, 2011) and simple pitch sequence processing in melody (Rogalsky et al., 2011; Stewart, Overath, Warren, Foxton, & Griffiths, 2008; Brattico, Tervaniemi, Näätänen, & Peretz, 2006; Patterson, Uppenkamp, Johnsrude, & Griffiths, 2002). Acquired musical perception deficits are associated with primarily posterior STG damage (Stewart, von Kriegstein, Warren, & Griffiths, 2006), and musical training is associated with changes in this region (Hyde et al., 2009). These results are consistent with our finding that the posterior STG was recruited for musical processing overall but not differentially recruited for different cadence types. Anterior regions of the STG and IFG are typically recruited for chord progressions and natural music with harmonic content (i.e., pieces with multiple voices; Caria, Venuti, & de Falco, 2011; Koelsch, Fritz, et al., 2005). Harmonized music differs from simple melody and isolated chords in a number of salient ways. It requires processing more acoustic information overall, tracking tones both horizontally (across time) and vertically (simultaneously in time), and interpreting the piece in light of previously learned harmonic structure of the musical system. Recruitment of anterior STG for harmonic processing is consistent with studies showing hierarchical organization of the STG, with anterior regions representing more complex information (Chevillet, Riesenhuber, & Rauschecker, 2011). Garza Villarreal et al. (2011) characterized the difference between regions as the posterior STG detecting sequential scale regularities and the IFG parsing hierarchical regularities.

Conclusion

Our study contributes to the understanding of the neural bases of music by mapping, for the first time, a cortico-BG network underling harmonic expectancy processing. It contributes to the understanding of music as embodying development of tension and resolution and relates these functions in a broader context, as one of many several types of cognitive expectancy. Specifically, this study provides evidence for the BG's role in processing musical expectation violation. It supports the view that inferior frontal and anterior superior temporal regions, previously linked to processing linguistic syntax, are also involved in processing musical syntax, and suggests differences in the contributions of the anterior and posterior STG to music perception. Finally, our study contributes a broader trend within cognitive neuroscience toward an increased appreciation of the predictive nature of many neural systems (Friston & Kiebel, 2009; Summerfield & Egner, 2009).

Reprint requests should be sent to Carol A. Seger, Department of Psychology, 1876 Campus Delivery, Colorado State University, Fort Collins, CO 80523, or via e-mail: Carol.Seger@colostate.edu.

Note

1.   This region was more active overall in Music Baseline > All Cadences contrast, which was the opposite direction of activity than the other two ROIs.

REFERENCES

Alexander, G. E., DeLong, M. R., & Strick, P. L. (1986). Parallel organization of functionally segregated circuits linking basal ganglia and cortex. *Annual Review of Neuroscience, 9,* 357–381.

Alluri, V., Toiviainen, P., Jääskeläinen, I. P., Glerean, E., Sams, M., & Brattico, E. (2012). Large-scale brain networks emerge from dynamic processing of musical timbre, key and rhythm. *Neuroimage, 59,* 3677–3689.

Andrews-Hanna, J. R., Reidler, J. S., Huang, C., & Buckner, R. L. (2010). Evidence for the default network's role in spontaneous cognition. *Journal of Neurophysiology, 104,* 322–335.

Ashby, F. G., Turner, B. O., & Horvitz, J. C. (2010). Cortical and basal ganglia contributions to habit learning and automaticity. *Trends in Cognitive Sciences, 14,* 208–215.

Bahlmann, J., Schubotz, R. I., & Friederici, A. D. (2008). Hierarchical artificial grammar processing engages Broca's area. *Neuroimage, 42,* 525–534.

Bahlmann, J., Schubotz, R. I., Mueller, J. L., Koester, D., & Friederici, A. D. (2009). Neural circuits of hierarchical visuo-spatial sequence processing. *Brain Research, 1298C,* 161–170.

Brattico, E., Tervaniemi, M., Näätänen, R., & Peretz, I. (2006). Musical scale properties are automatically processed in the human auditory cortex. *Brain Research, 1117,* 162–174.

Braunlich, K., & Seger, C. A. (2013). Basal ganglia. *Wiley Interdisciplinary Reviews: Cognitive Science, 4,* 135–148.

Brennan, J., Niv, Y., Hasson, U., Malach, R., Heeger, D. J., & Pylkkänen, L. (2012). Syntactic structure building in the anterior temporal lobe during natural story listening. *Brain and Language, 120,* 163–173.

Bromberg-Martin, E. S., Matsumoto, M., & Hikosaka, O. (2010). Dopamine in motivational control: Rewarding, aversive, and alerting. *Neuron, 68,* 815–834.

Burzynska, A. Z., Nagel, I. E., Preuschhof, C., Li, S. C., Lindenberger, U., Bäckman, L., et al. (2011). Microstructure of frontoparietal connections predicts cortical responsivity and working memory performance. *Cerebral Cortex, 21,* 2261–2271.

Caria, A., Venuti, P., & de Falco, S. (2011). Functional and dysfunctional brain circuits underlying emotional processing of music in autism spectrum disorders. *Cerebral Cortex, 21,* 2838–2849.

Chen, J. L., Penhune, V. B., & Zatorre, R. J. (2008). Listening to musical rhythms recruits motor regions of the brain. *Cerebral Cortex, 18,* 2844–2854.

Chevillet, M., Riesenhuber, M., & Rauschecker, J. P. (2011). Functional correlates of the anterolateral processing hierarchy in human auditory cortex. *Journal of Neuroscience, 31,* 9345–9352.

Doeller, C. F., Opitz, B., Mecklinger, A., Krick, C., Reith, W., & Schröger, E. (2003). Prefrontal cortex involvement in preattentive auditory deviance detection: Neuroimaging and electrophysiological evidence. *Neuroimage, 20,* 1270–1282.

Forman, S. D., Cohen, J. D., Fitzgerald, M., Eddy, W. F., Mintun, M. A., & Noll, D. C. (1995). Improved assessment of significant activation in functional magnetic resonance imaging (fMRI): Use of a cluster-size threshold. *Magnetic Resonance in Medicine, 33,* 636–647.

Frank, M. J. (2011). Computational models of motivated action selection in corticostriatal circuits. *Current Opinion in Neurobiology, 21,* 381–386.

Friederici, A. D. (2009). Pathways to language: Fiber tracts in the human brain. *Trends in Cognitive Sciences, 13,* 175–181.

Friston, K., & Kiebel, S. (2009). Predictive coding under the free-energy principle. *Philosophical Transactions of the Royal Society of London, Series B, Biological Sciences, 364,* 1211–1221.

Fujisawa, T. X., & Cook, N. D. (2011). The perception of harmonic triads: An fMRI study. *Brain Imaging and Behavior, 5,* 109–125.

Garza Villarreal, E. A., Brattico, E., Leino, S., Ostergaard, L., & Vuust, P. (2011). Distinct neural responses to chord violations: A multiple source analysis study. *Brain Research, 1389,* 103–114.

Glimcher, P. W. (2011). Understanding dopamine and reinforcement learning: The dopamine reward prediction error hypothesis. *Proceedings of the National Academy of Sciences, U.S.A., 108(Suppl. 3),* 15647–15654.

Goebel, R., Esposito, F., & Formisano, E. (2006). Analysis of functional image analysis contest (FIAC) data with brainvoyager QX: From single-subject to cortically aligned group general linear model analysis and self-organizing group independent component analysis. *Human Brain Mapping, 27,* 392–401.

Grahn, J. A., & Rowe, J. B. (2009). Feeling the beat: Premotor and striatal interactions in musicians and nonmusicians during beat perception. *Journal of Neuroscience, 29,* 7540–7548.

Groussard, M., Rauchs, G., Landeau, B., Viader, F., Desgranges, B., Eustache, F., et al. (2010). The neural substrates of musical memory revealed by fMRI and two semantic tasks. *Neuroimage, 53,* 1301–1309.

Haber, S. N. (2003). The primate basal ganglia: Parallel and integrative networks. *Journal of Chemical Neuroanatomy, 26,* 317–330.

Huron, D. (2006). *Sweet anticipation: Music and the psychology of expectation*. Cambridge, MA: MIT Press.

Hyde, K. L., Lerch, J., Norton, A., Forgeard, M., Winner, E., Evans, A. C., et al. (2009). Musical training shapes structural brain development. *Journal of Neuroscience, 29,* 3019–3025.

Hyde, K. L., Zatorre, R. J., & Peretz, I. (2011). Functional MRI evidence of an abnormal neural network for pitch processing in congenital amusia. *Cerebral Cortex, 21,* 292–299.

Janata, P. (2009). The neural architecture of music-evoked autobiographical memories. *Cerebral Cortex, 19,* 2579–2594.

Janata, P., Birk, J. L., Van Horn, J. D., Leman, M., Tillmann, B., & Bharucha, J. J. (2002). The cortical topography of tonal structures underlying Western music. *Science, 298,* 2167–2170.

Janata, P., & Grafton, S. T. (2003). Swinging in the brain: Shared neural substrates for behaviors related to sequencing and music. *Nature Neuroscience, 6,* 682–687.

Jerde, T. A., Childs, S. K., Handy, S. T., Nagode, J. C., & Pardo, J. V. (2011). Dissociable systems of working memory for rhythm and melody. *Neuroimage, 57,* 1572–1579.

Klein, M. E., & Zatorre, R. J. (2011). A role for the right superior temporal sulcus in categorical perception of musical chords. *Neuropsychologia, 49,* 878–887.

Koelsch, S. (2011). Toward a neural basis of music perception—A review and updated model. *Frontiers in Psychology, 2,* 110.

Koelsch, S., Fritz, T., & Schlaug, G. (2008). Amygdala activity can be modulated by unexpected chord functions during music listening. *NeuroReport, 19,* 1815–1819.

Koelsch, S., Fritz, T., Schulze, K., Alsop, D., & Schlaug, G. (2005). Adults and children processing music: An fMRI study. *Neuroimage, 25,* 1068–1076.

Koelsch, S., Gunter, T. C., von Cramon, D. Y., Zysset, S., Lohmann, G., & Friederici, A. D. (2002). Bach speaks: A cortical "language-network" serves the processing of music. *Neuroimage, 17,* 956–966.

Koelsch, S., Gunter, T. C., Wittfoth, M., & Sammler, D. (2005). Interaction between syntax processing in language and in music: An ERP study. *Journal of Cognitive Neuroscience, 17,* 1565–1577.

Kranjec, A., Cardillo, E. R., Schmidt, G. L., Lehet, M., & Chatterjee, A. (2012). Deconstructing events: The neural bases for space, time, and causality. *Journal of Cognitive Neuroscience, 24,* 1–16.

Kriegeskorte, N., Simmons, W. K., Bellgowan, P. S., & Baker, C. I. (2009). Circular analysis in systems neuroscience: The dangers of double dipping. *Nature Neuroscience, 12,* 535–540.

Krumhansl, C. L., & Cuddy, L. L. (2010). A theory of tonal hierarchies in music. In M. R. Jones et al. (Eds.), *Music perception, Springer handbook of auditory research* (p. 36). New York: Springer.

Langner, R., Kellermann, T., Eickhoff, S. B., Boers, F., Chatterjee, A., Willmes, K., et al. (2012). Staying responsive to the world: Modality-specific and −nonspecific contributions to speeded auditory, tactile, and visual stimulus detection. *Human Brain Mapping, 33,* 398–418.

Lawrence, A. D., Sahakian, B. J., & Robbins, T. W. (1998). Cognitive functions and corticostriatal circuits: Insights from Huntington's disease. *Trends in Cognitive Sciences, 2,* 379–388.

Lebrun-Guillaud, G., Tillmann, B., & Justus, T. (2008). Perception of tonal and temporal structures in chord sequences by patients with cerebellar damage. *Music Perception, 25,* 271–283.

Lee, D., Seo, H., & Jung, M. W. (2012). Neural basis of reinforcement learning and decision making. *Annual Review of Neuroscience, 35,* 287–308.

Lee, Y. S., Janata, P., Frost, C., Hanke, M., & Granger, R. (2011). Investigation of melodic contour processing in the brain using multivariate pattern-based fMRI. *Neuroimage, 57,* 293–300.

Lerdahl, F., & Jackendoff, R. S. (1996). *A generative theory of tonal music*. Cambridge, MA: MIT Press.

Levitin, D. J., & Tirovolas, A. K. (2009). Current advances in the cognitive neuroscience of music. *Annals of the New York Academy of Sciences, 1156,* 211–231.

Lohrenz, T., McCabe, K., Camerer, C. F., & Montague, P. R. (2007). Neural signature of fictive learning signals in a sequential investment task. *Proceedings of the National Academy of Sciences, U.S.A., 104,* 9493–9498.

Lopez-Barroso, D., de Diego-Balaguer, R., Cunillera, T., Camara, E., Münte, T. F., & Rodriguez-Fornells, A. (2011). Language learning under working memory constraints correlates with microstructural differences in the ventral language pathway. *Cerebral Cortex, 21,* 2742–2750.

Lopez-Paniagua, D., & Seger, C. A. (2011). Interactions within and between corticostriatal loops during component processes of category learning. *Journal of Cognitive Neuroscience, 23,* 3068–3083.

Loui, P., Li, H. C., & Schlaug, G. (2011). White matter integrity in right hemisphere predicts pitch-related grammar learning. *Neuroimage, 55,* 500–507.

Maess, B., Koelsch, S., Gunter, T. C., & Friederici, A. D. (2001). Musical syntax is processed in Broca's area: An MEG study. *Nature Neuroscience, 4,* 540–545.

Maidhof, C., & Koelsch, S. (2011). Effects of selective attention on syntax processing in music and language. *Journal of Cognitive Neuroscience, 23,* 2252–2267.

Makuuchi, M., Bahlmann, J., Anwander, A., & Friederici, A. D. (2009). Segregating the core computational faculty of human language from working memory. *Proceedings of the National Academy of Sciences, U.S.A., 106,* 8362–8367.

Meyer, L. (1989). *Style and music: Theory, history, and ideology*. Chicago: University of Chicago Press.

Montag, C., Reuter, M., & Axmacher, N. (2011). How one's favorite song activates the reward circuitry of the brain: Personality matters! *Behavioural Brain Research, 225,* 511–514.

Mueller, K., Mildner, T., Fritz, T., Lepsien, J., Schwarzbauer, C., Schroeter, M. L., et al. (2011). Investigating brain response to music: A comparison of different fMRI acquisition schemes. *Neuroimage, 54,* 337–343.

Nee, D. E., Kastner, S., & Brown, J. W. (2011). Functional heterogeneity of conflict, error, task-switching, and unexpectedness effects within medial prefrontal cortex. *Neuroimage, 54,* 528–540.

Opitz, B., & Friederici, A. D. (2007). Neural basis of processing sequential and hierarchical syntactic structures. *Human Brain Mapping, 28,* 585–592.

Parsons, L. M., Petacchi, A., Schmahmann, J. D., & Bower, J. M. (2009). Pitch discrimination in cerebellar patients: Evidence for a sensory deficit. *Brain Research, 1303,* 84–96.

Patel, A. D. (2003). Language, music, syntax and the brain. *Nature Neuroscience, 6,* 674–681.

Patterson, R. D., Uppenkamp, S., Johnsrude, I. S., & Griffiths, T. D. (2002). The processing of temporal pitch and melody information in auditory cortex. *Neuron, 36,* 767–776.

Pearce, M. T., Ruiz, M. H., Kapasi, S., Wiggins, G. A., & Bhattacharya, J. (2009). Unsupervised statistical learning underpins computational, behavioural, and neural manifestations of musical expectation. *Neuroimage, 50,* 302–313.

Perani, D., Saccuman, M. C., Scifo, P., Awander, A., Spada, D., Baldoli, C., et al. (2011). Neural language networks at birth.

Proceedings of the National Academy of Sciences, U.S.A., 108, 16056–16061.

Peretz, I., Brattico, E., Järvenpää, M., & Tervaniemi, M. (2009). The amusic brain: In tune, out of key, and unaware. *Brain, 132,* 1277–1286.

Peterson, E. J., & Seger, C. A. (in press). Many hats: Intra-trial and reward-level dependent BOLD activity in the striatum and premotor cortex. *Journal of Neurophysiology*.

Poldrack, R. A., & Mumford, J. A. (2009). Independence in ROI analysis: Where is the voodoo? *Social Cognitive and Affective Neuroscience, 4,* 208–213.

Roebroeck, A., Formisano, E., & Goebel, R. (2005). Mapping directed influence over the brain using Granger causality and fmri. *Neuroimage, 25,* 230–242.

Rogalsky, C., Rong, F., Saberi, K., & Hickok, G. (2011). Functional anatomy of language and music perception: Temporal and structural factors investigated using functional magnetic resonance imaging. *Journal of Neuroscience, 31,* 3843–3852.

Salimpoor, V. N., Benovoy, M., Larcher, K., Dagher, A., & Zatorre, R. J. (2011). Anatomically distinct dopamine release during anticipation and experience of peak emotion to music. *Nature Neuroscience, 14,* 257–262.

Santi, A., & Grodzinsky, Y. (2010). fMRI adaptation dissociates syntactic complexity dimensions. *Neuroimage, 51,* 1285–1293.

Schiffer, A. M., & Schubotz, R. I. (2011). Caudate nucleus signals for breaches of expectation in a movement observation paradigm. *Frontiers in Human Neuroscience, 5,* 38.

Schlaug, G., Marchina, S., & Norton, A. (2009). Evidence for plasticity in white-matter tracts of patients with chronic Broca's aphasia undergoing intense intonation-based speech therapy. *Annals of the New York Academy of Sciences, 1169,* 385–394.

Schulze, K., Zysset, S., Mueller, K., Friederici, A. D., & Koelsch, S. (2010). Neuroarchitecture of verbal and tonal working memory in nonmusicians and musicians. *Human Brain Mapping, 32,* 771–783.

Schwartze, M., Keller, P. E., Patel, A. D., & Kotz, S. A. (2011). The impact of basal ganglia lesions on sensorimotor synchronization, spontaneous motor tempo, and the detection of tempo changes. *Behavioural Brain Research, 216,* 685–691.

Seger, C. A. (2008). How do the basal ganglia contribute to categorization? Their roles in generalization, response selection, and learning via feedback. *Neuroscience and Biobehavioral Reviews, 32,* 265–278.

Seger, C. A. (2009). The involvement of corticostriatal loops in learning across tasks, species, and methodologies. In H. J. Groenewegen, P. Voorn, H. W. Berendse, A. B. Mulder, A. R. Cools (Eds.), *Basal ganglia IX: Proceedings of the International Basal Ganglia Society* (pp. 25–40). New York, NY: Springer.

Seger, C. A., Dennison, C. S., Lopez-Paniagua, D., Peterson, E. J., & Roark, A. A. (2011). Dissociating hippocampal and basal ganglia contributions to category learning using stimulus novelty and subjective judgments. *Neuroimage, 55,* 1739–1753.

Seger, C. A., Peterson, E. J., Cincotta, C. M., Lopez-Paniagua, D., & Anderson, C. W. (2010). Dissociating the contributions of independent corticostriatal systems to visual categorization learning through the use of reinforcement learning modeling and Granger causality modeling. *Neuroimage, 50,* 644–656.

Smith, S. M., Miller, K. L., Salimi-Khorshidi, G., Webster, M., Beckmann, C. F., Nichols, T. E., et al. (2011). Network modelling methods for fMRI. *Neuroimage, 54,* 875–891.

Stewart, L., Overath, T., Warren, J. D., Foxton, J. M., & Griffiths, T. D. (2008). fMRI evidence for a cortical hierarchy of pitch pattern processing. *Plos One, 3,* e1470.

Stewart, L., von Kriegstein, K., Warren, J. D., & Griffiths, T. D. (2006). Music and the brain: Disorders of musical listening. *Brain, 129,* 2533–2553.

Summerfield, C., & Egner, T. (2009). Expectation (and attention) in visual cognition. *Trends in Cognitive Sciences, 13,* 403–409.

Sutton, R. S., & Barto, A. G. (1998). *Reinforcement learning: An introduction.* Cambridge, MA: MIT Press.

Talairach, J., & Tournoux, P. (1998). *Co-planar stereotaxic atlas of the human brain: 3-Dimensional proportional system—An approach to cerebral imaging.* New York: Thieme.

Thaut, M. H., Stephan, K. M., Wunderlich, G., Schicks, W., Tellmann, L., Herzog, H., et al. (2009). Distinct cortico-cerebellar activations in rhythmic auditory motor synchronization. *Cortex, 45,* 44–53.

Tillman, B. (2008). Music Cognition: Learning, Perception, Expectations. In R. Kronland-Martinet, S. Ystad, and K. Jensen (Eds.), *CMMR 2007, LNCS 4969,* pp. 11–33.08

Tritsch, N. X., & Sabatini, B. L. (2012). Dopaminergic modulation of synaptic transmission in cortex and striatum. *Neuron, 76,* 33–50.

Vuust, P., & Kringelbach, M. L. (2010). The pleasure of making sense of music. *Interdisciplinary Science Reviews, 35,* 166–182.

Vuust, P., Wallentin, M., Mouridsen, K., Ostergaard, L., & Roepstorff, A. (2011). Tapping polyrhythms in music activates language areas. *Neuroscience Letters, 494,* 211–216.

Wilson, S. M., Galantucci, S., Tartaglia, M. C., Rising, K., Patterson, D. K., Henry, M. L., et al. (2011). Syntactic processing depends on dorsal language tracts. *Neuron, 72,* 397–403.

Yeterian, E. H., & Pandya, D. N. (1998). Corticostriatal connections of the superior temporal region in rhesus monkeys. *Journal of Comparative Neurology, 399,* 384–402.

Zacks, J. M., Kurby, C. A., Eisenberg, M. L., & Haroutunian, N. (2011). Prediction error associated with the perceptual segmentation of naturalistic events. *Journal of Cognitive Neuroscience, 23,* 4057–4066.

Zatorre, R. J., Chen, J. L., & Penhune, V. B. (2007). When the brain plays music: Auditory-motor interactions in music perception and production. *Nature Reviews Neuroscience, 8,* 547–558.